Letter

Experimental optimization of charging quantum batteries through a catalyst system

Dengke Qu [1,*] Xiang Zhan [2,*] Haiqing Lin,[3] and Peng Xue [1,†]

[1] *Beijing Computational Science Research Center, Beijing 100193, China*

[2] *School of Physics and MIIT Key Laboratory of Semiconductor Microstructure and Quantum Sensing, Nanjing University of Science and Technology, Nanjing 210094, China*

[3] *School of Physics, Zhejiang University, Hangzhou 310030, China*

(Received 13 June 2023; revised 15 August 2023; accepted 17 October 2023; published 2 November 2023)

Quantum batteries are quantum systems that potentially serve as fuel for other quantum devices by receiving and supplying energy. In this Letter, we investigate the charging processes of a state-of-the-art quantum battery made of a harmonic oscillator, which can store infinite amounts of energy in principle. We experimentally simulate the charging process using a high-dimensional photonic quantum system with multiple concatenated interferometers. Our experiments demonstrate that both the stored and extractable energy of the quantum battery can be significantly improved by introducing a catalyst system. This charging protocol has the same performance as optimized the frequency of the external field in the direct charging protocol but is more convenient without the requirement of probing the global frequency of the charge-battery system. From the viewpoint of experimental innovation, we propose a general method to deterministically implement an arbitrary trace-preserving nonunitary channel and realize it experimentally. Our work shows the potential of this interesting quantum battery and sheds light on experimental investigations of quantum batteries.

DOI: 10.1103/PhysRevB.108.L180301

Introduction. Thermodynamics forms the cornerstone of our current understanding of the physical world, which has traditionally been concerned with low-speed macroscopic systems. Along with representative revolutions in relativity and quantum theory, thermodynamics has been applied beyond its original domain, from the study of black holes [1,2] to quantum thermodynamics [3,4]. Quantum thermodynamics focuses on explaining thermodynamic concepts such as energy, work, and entropy, in the quantum world [5–11]. To this end, quantum batteries (QBs) [12–17], quantum systems for receiving and supplying energy, have emerged as a powerful paradigm to explore the laws and potential applications of energy transmission by utilizing quantum resources such as entanglement [18–20], coherence [21–25], and discord [26–28].

The task to optimize a QB includes improving the storage of energy during charging, as well as enhancing the ability to transfer the stored energy to the center of consumption during discharging [29–37]. For traditional QBs made of n two-level systems, there are a series of protocols to exploit the stored energy through parallel charging [38–40] or collective charging [39–43]. Here, we consider a different model of the QB made by quantum harmonic oscillators (QHOs) [44–46], which we refer to as a quantum harmonic oscillator battery (QHOB). Compared with a two-level system whose maximum stored energy is limited to one quanta, a QHOB can in principle store an arbitrary amount of energy.

In this Letter, we consider a QHOB charged by another QHO (charger) driven by an external laser field. We simulate the charging process of the QHOB using a single-photon interference network. To improve the energy storage of the QHOB, we employ two optimization schemes, either by tuning the frequency of the charging laser field or introducing a catalyst system. Furthermore, we investigate the effect of the temperature of the environment on energy extraction. We evaluate the robust performance of the QHOB when energy is dissipated from the charger and catalyst system to the environment. Our work provides an experimental demonstration of charging quantum batteries through a catalyst system. In addition, from the viewpoint of experimental innovation, we propose a general method to deterministically implement trace-preserving nonunitary channels and realize it experimentally through a single-photon interferometric network.

Model. A straightforward method for charging the QHOB is shown in Fig. 1(a). Here, the QHOB with frequency ω_b is directly charged by another QHO with frequency ω_c, which is coupled with the external laser field of frequency ω_f and amplitude F [33,45]. Therefore, we call this charging process a direct charging process, of which the Hamiltonian of the whole system is ($\hbar = 1$)

$$H = \omega_c c^\dagger c + \omega_b b^\dagger b + g_{cb}(cb^\dagger + c^\dagger b) + F(e^{i\omega_f t} c + e^{-i\omega_f t} c^\dagger), \tag{1}$$

where g_{cb} is the coupling strength between the battery and the charger, and b ($b^\dagger$) and c ($c^\dagger$) are the annihilation (creation) operators of the battery and the charger, respectively.

At the beginning time $t = 0$, the whole system is initialized in a product state $\rho_{cb}(0)$ with both the charger and the battery

[*] These authors contributed equally to this work.

[†] gnep.eux@gmail.com

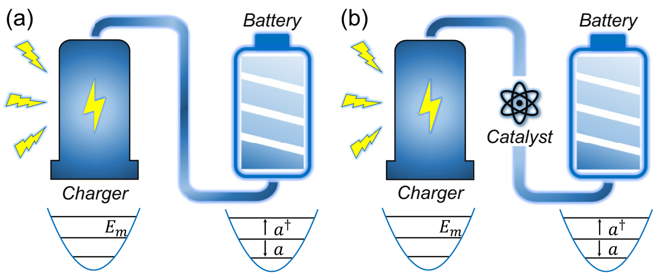

FIG. 1. Schematic illustration of two charging protocols for the QHOB. (a) The QHOB is directly coupled to the charger, which is driven by an external laser field. (b) A two-level quantum system acts as a catalyst system between the QHOB and the charger.

being in their ground states. In order to transfer energy to a traditional QB, the charger is generally required to be prepared in a specific initial state [42–44], but this requirement can be avoided in our charging protocols. Considering that the energy of the charger is dissipated to the environment during charging, the dynamics of the direct charging process can be described by the Lindblad form master equation as [47]

$$\begin{aligned}\frac{d\rho_{cb}}{dt} =& -i[g_{cb}(cb^\dagger + c^\dagger b) + F(e^{i\Delta t}c + e^{-i\Delta t}c^\dagger), \rho_{cb}]\\ &+ \gamma_c[N(T)+1]\mathcal{D}_c[\rho_{cb}] + \gamma_c N(T)\mathcal{D}_{c^\dagger}[\rho_{cb}],\end{aligned} \tag{2}$$

where $\mathcal{D}_x[\rho] = x\rho x^\dagger - \{x^\dagger x, \rho\}/2$ denotes the dissipator, γ_c is the rate of spontaneous emission, $N(T) = 1/(e^{\omega/kT} - 1)$ represents the average photon number in mode ω of the environment at temperature T, k is the Boltzmann constant, and $\Delta = \omega_f - \omega_c$ is the detuning between the laser field and the charger. Let us assume that the battery and charger are in resonance with $\omega_c = \omega_b = \omega$.

For the direct charging protocol, the system Hamiltonian can be rewritten as

$$\begin{aligned}H =& \omega_+ C_+^\dagger C_+ + \omega_- C_-^\dagger C_- + \frac{F}{\sqrt{2}}(e^{i\omega_f t}C_+ + e^{-i\omega_f t}C_+^\dagger)\\ &+ \frac{F}{\sqrt{2}}(e^{i\omega_f t}C_- + e^{-i\omega_f t}C_-^\dagger),\end{aligned} \tag{3}$$

where $C_\pm = \frac{1}{\sqrt{2}}(c \pm b)$ represent the global supermode operators and $\omega_\pm = \omega \pm g_{cb}$. This equation shows that when the frequency of the laser field is adjusted to $\omega_\pm$, it will resonate with the global modes $C_\pm$ of the battery charger, thereby breaking through the charging limit of the quantum battery.

Inspired by the study of catalysts in quantum thermodynamics [48–58], let us consider another charging process assisted by catalysts, which we refer to as catalyst-assisted charging. More specifically, we add a two-level quantum system (catalysts) between the charger and the battery, resulting in no direct interaction between them, as shown in Fig. 1(b). In this case, the Hamiltonian of the whole system becomes

$$\begin{aligned}H =& \omega c^\dagger c + \omega_q q^\dagger q + \omega b^\dagger b + g_{cq}(cq^\dagger + c^\dagger q)\\ &+ g_{bq}(bq^\dagger + b^\dagger q) + F(e^{i\omega_f t}c + e^{-i\omega_f t}c^\dagger),\end{aligned} \tag{4}$$

where g_{cq} (g_{bq}) is the coupling strength between the charger (battery) and the catalyst and $q = 1/2(\sigma_x + i\sigma_y)$ ($q^\dagger$) represents the annihilation (creation) operator of the catalyst.

For the catalyst-assisted charging protocol, the system Hamiltonian can be rewritten as

$$\begin{aligned}H =& \omega C_+^\dagger C_+ + \omega C_-^\dagger C_- + \omega_q q^\dagger q + g(C_+ q^\dagger + C_+^\dagger q)\\ &+ F\sin\theta(e^{i\omega_f t}C_+ + e^{-i\omega_f t}C_+^\dagger)\\ &+ F\cos\theta(e^{i\omega_f t}C_- + e^{-i\omega_f t}C_-^\dagger),\end{aligned}$$

where the supermode operators $C_+ = \sin\theta c + \cos\theta b$ and $C_- = \cos\theta c - \sin\theta b$ with $\sin\theta = g_{cq}/g$, $\cos\theta = g_{bq}/g$, and $g = \sqrt{g_{cq}^2 + g_{bq}^2}$. Even if the laser frequency is $\omega_f = \omega$, the laser field resonates with the global mode C_- of the charger-battery system, enabling unlimited energy transfer without relying on the energy splitting ω_q of the catalyst and the coupling constant g_{cq} and g_{bq} [45]. For convenience, we also set all frequencies to ω. Considering the energy dissipation of the charger and the catalyst, the dynamics of the charging process is described by the master equation as

$$\begin{aligned}\frac{d\rho_{cbq}}{dt} =& -i[g(cq^\dagger + c^\dagger q + bq^\dagger + b^\dagger q) + F(c + c^\dagger), \rho_{cbq}]\\ &+ \sum_{x=c,q}\gamma_x\{[N(T)+1]\mathcal{D}_x[\rho_{cbq}] + N(T)\mathcal{D}_{x^\dagger}[\rho_{cbq}]\},\end{aligned} \tag{5}$$

where $g = \sqrt{g_{cq}^2 + g_{bq}^2}$.

The energy stored in the battery state $\rho_b(t)$ at time t is given by

$$E_b(t) = \mathrm{Tr}[b^\dagger b\rho_b(t)]. \tag{6}$$

We quantify the extractable work using ergotropy [22,59], which represents the maximum energy that can be extracted with any cyclic unitary transformation. Sorting the labels of eigenstates of the $b^\dagger b = \sum_{n=1}^d \epsilon_n|\epsilon_n\rangle\langle\epsilon_n|$ and $\rho_b(t) = \sum_{n=1}^d r_n|r_n\rangle\langle r_n|$ according to the rules of $\epsilon_n < \epsilon_{n+1}$ and $r_n > r_{n+1}$, the optimal ergotropic transformation [22] can be defined to map the battery state to the passive state $\rho_p(t) = \sum_{n=1}^d r_n|\epsilon_n\rangle\langle\epsilon_n|$. Then, the ergotropy is given by

$$W_e(t) = E_b(t) - E_p(t), \tag{7}$$

where $E_p(t) = \mathrm{Tr}[b^\dagger b\rho_p(t)]$. The energy occupied by the catalyst is $E_q(t) = \mathrm{Tr}[q^\dagger q\rho_q(t)]$, where $\rho_q(t)$ is the state of the catalyst. We refer to the energy in the catalyst as residual energy, which is used to measure the performance of the catalyst.

Quantum channel of the charging process. To simulate the charging process, we transform the description of the process in the master equation into an equivalent but more visualized description as the quantum channel [60]. Since we are only concerned about the performance of the QHOB and the impact of catalysts on them, we only consider the dynamics of the open quantum system without the charger, which we deal with as an environment. Therefore, both charging processes can be described by a quantum channel in the operator-sum representation as

$$\rho_x(t) = \mathcal{E}_t[\rho_x(0)] = \sum_{n=1}^{d^2} K_n(t)\rho_x(0)K_n^\dagger(t), \tag{8}$$

where $x = b$ (bq) represents the QHOB (QHOB and catalyst) system for direct (catalyst-assisted) charging, $K_n(t)$ is a time-dependent Kraus operator, and d denotes the dimension of the whole system. Generally, the quantum channel $\mathcal{E}_t$ is trace preserving but not random unitary, that is $\sum_{n=1}^{d^2} \mathrm{Tr}[K_n(t)\rho_x(0)K_n^\dagger(t)] = 1$ and the Kraus operator $K_n(t)$ is not proportional to any unitary operator.

To deterministically realize these channels, we propose a general method, which uses an ancillary qubit initialized in state $|1\rangle$. Let us denote the nonunitary operators as $K_n(t) = \sum_{m=1}^{d} |m\rangle\langle\psi_{n,m}|$, where $|\psi_{n,m}\rangle$ is the unnormalized states whose normalized form is $|\bar{\psi}_{n,m}\rangle = |\psi_{n,m}\rangle/\||\psi_{n,m}\rangle\|$. The method iteratively does the following procedures for $n = 1, \dots, d^2$: For each n, iteratively implement $B_{n,m}A_{n,m}$ for $m = d, \dots, 1$ and then measure the ancillary qubit in the basis $|0\rangle\langle 0|$. Here, $A_{n,m}$ and $B_{n,m}$ are the ancilla-control-system and system-control-ancilla operations as

$$\begin{aligned} A_{n,m} &= |1\rangle\langle 1| \otimes C_{n,m} + |0\rangle\langle 0| \otimes \mathbb{1}_d, \\ B_{n,m} &= S_{n,m} \otimes |m\rangle\langle m| + \mathbb{1}_2 \otimes (\mathbb{1}_d - |m\rangle\langle m|), \end{aligned} \tag{9}$$

respectively, where $S_{n,m} = (r_{n,m}\sigma_x - t_{n,m}\sigma_z)$ with $r_{n,m} = \||\psi_{n,m}\rangle\| \times \|\langle\bar{\psi}_{n,m}|L_{n,m+1}^+\|$ and $t_{n,m} = \sqrt{1 - r_{n,m}^2}$, $C_{n,m}$ is a unitary operator that satisfies

$$\langle j|C_{n,m} = \frac{\langle\bar{\psi}_{n,m}|L_{n,m+1}^+}{\|\langle\bar{\psi}_{n,m}|L_{n,m+1}^+\|}, \tag{10}$$

where the operator $L_{n,m}$ is defined as $L_{n,m} = [\mathbb{1}_d - (1 - t_{n,m})|m\rangle\langle m|]C_{n,m}L_{n,m+1}$ with $L_{n,d+1} = \mathbb{1}_d$ and the superscript $+$ denotes the Moore-Penrose inverse [61]. Once the measurement gives a positive outcome, the procedure is finished, otherwise, the ancillary qubit collapses to state $|1\rangle$ and the whole procedure moves to the next iteration with a larger n. Specifically, when ancillary qubit collapses to state $|0\rangle$, the transformation of the system can be expressed as

$$\begin{aligned} T_n &= \sum_{m=1}^{d} r_{n,m}|m\rangle\langle m|C_{n,m}L_{n,m+1} \\ &= \sum_{m=1}^{d} \frac{r_{n,m}}{\|\langle\bar{\psi}_{n,m}|L_{n,m+1}^+\|}|m\rangle\langle\bar{\psi}_{n,m}|L_{n,m+1}^+L_{n,m+1} \\ &= \sum_{m=1}^{d} |m\rangle\langle\psi_{n,m}| = K_n. \end{aligned} \tag{11}$$

This procedure will stop after iteration number n with probability $\mathrm{Tr}[K_n\rho_x(0)K_n^\dagger]$ and leave the state being $K_n\rho_x(0)K_n^\dagger/\mathrm{Tr}[K_n\rho_x(0)K_n^\dagger]$. Since the channel is trace preserving, this procedure must be stopped within d^2 iterations. Thereby it is a deterministic procedure. Thus, this method is general and can be used to implement an arbitrary trace-preserving channel.

Experimental implementation. We experimentally simulate the two charging processes with single photons and linear optics as shown in Fig. 2(a). In our simulation, we truncate the infinite-dimensional space of the QHO into a finite-dimensional space [62,63]. In particular, we set the maximum photon number as 3. Therefore, the truncated QHOB and battery-catalyst systems are four- and eight-dimensional qudits, respectively.

For the direct charging process, we encode the basis of the four-dimensional qudit as $|0\rangle = |P_1H\rangle, |1\rangle = |P_1V\rangle, |2\rangle = |P_2H\rangle, |3\rangle = |P_2V\rangle$, where P_i represents the ith spatial mode and H (V) represents the horizontal (vertical) polarization of the photons. Furthermore, the basis $|1\rangle$ ($|0\rangle$) of the ancillary qubit is encoded by the original (additional) two spatial modes.

In our experiment, the initial state of the battery is prepared in the ground state $\rho_b(0) = |0\rangle\langle 0|$ by heralded single photons passing through a polarizing beam splitter (PBS). Then the ancilla-control-system operator $A_{n,m}$ is realized by performing the unitary operation $C_{n,m}$ on the original spatial mode while leaving the additional spatial mode unchanged. To realize the system-control-ancilla operation $B_{n,m}$, we split the original spatial mode into the additional spatial mode and then perform the unitary operation $S_{n,m}$. More specifically, since only one row of $C_{n,m}$ is specified, its realization can be realized by two beam displacers (BDs) and three half-wave plates (HWPs) [64,65]. The operator $S_{n,m}$ is realized only by one HWP. In principle, there are d^2 iterations to realize the channel of charging. However, to reduce the error accumulated in multiple experiments, we choose d' iterations that realize the channel $\rho_b'(t) = \sum_{n'=1}^{d'} K_{n'}(t)\rho_b(x)K_{n'}^\dagger(t)$, quite similar to the ideal one as $\mathrm{Tr}[\sqrt{\rho_b'(t)^{1/2}\rho_b(t)\rho_b'(t)^{1/2}}] > 0.99$.

The measurement of the ancillary qubit in the basis $|0\rangle\langle 0|$ corresponds to finding the photons in these additional spatial modes. In these modes, the state of the battery is constructed via quantum state tomography [66]. More specifically, we measure the photons in the basis $\{|P_0\rangle, |P_1\rangle, |P_+\rangle = (|P_0\rangle + |P_1\rangle)/\sqrt{2}, |P_-\rangle = (|P_0\rangle - i|P_1\rangle)/\sqrt{2}\} \otimes \{|H\rangle, |V\rangle, |+\rangle = (|H\rangle + |V\rangle)/\sqrt{2}, |-\rangle = (|H\rangle - i|V\rangle)/\sqrt{2}\}$ through the combination of wave plates (WPs), BD, and PBS, and then estimate the density matrix via maximumlike estimation. The outputs are recorded synchronously with the trigger photons.

The experiment for catalyst-assisted charging follows a similar procedure for direct charging. We encode the battery-catalyst system by eight-dimensional qudit as $\{|00\rangle = |P_1H\rangle, |10\rangle = |P_1V\rangle, |20\rangle = |P_2H\rangle, \dots, |31\rangle = |P_4V\rangle\}$. The initial state of the battery-catalyst system is prepared in the ground state by a PBS. At the arbitrary time t, the state of the battery $\rho_b(t)$ is obtained by discarding the catalyst system and performing two-qubit tomography. Furthermore, the residual energy of the catalyst, which corresponds to measurement $|1\rangle\langle 1|$, can be obtained by directly measuring the probability of the last four bases among all the basis.

Experimental results. To evaluate the performance of the QHOB, we have measured the stored energy and ergotropy during its charging process. As shown in Fig. 3(a), when the frequency of the laser field is straightforwardly chosen to be in resonance with both the charger and the battery, the stored energy has limitations for the environment of both zero temperature $N(T) = 0$ and nonzero temperature $N(T) = 1$. Interestingly, the energy storage in the zero-temperature

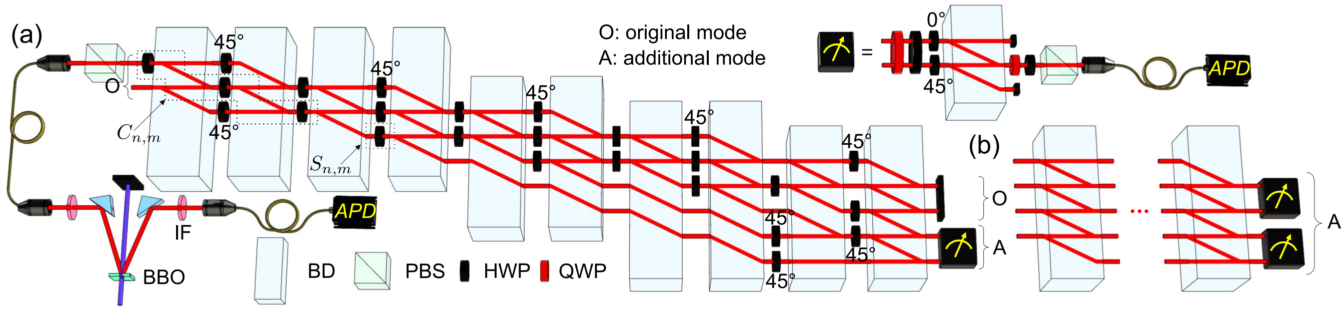

FIG. 2. Experimental setup for simulating (a) direct charging process and (b) catalyst-assisted charging process. A pair of photons are created via spontaneous parametric down-conversion, with one serving as a trigger and the other as a single photon. The ground state of the qudit is prepared by a PBS. Then the photons go through the optical network composed of WPs and BDs to realize the quantum channel of charging. Finally, measurements of the system are performed on the additional modes corresponding to the ancillary qubit at state $|0\rangle$. The signal photon is detected by avalanche photodiodes, and in typical measurements, there are a maximum of 10^4 photon counts over 2 s.

environment is always smaller than that in the nonzero-temperature environment, and the maximum values of the two are 0.812 ± 0.007 and 0.984 ± 0.009, respectively. At the time $t = 100$, the stored energy of the former even reached 0.209 ± 0.003 times that of the latter. This phenomenon is a bit abnormal because intuitively, the performance at zero temperature should be better. However, the benefit of zero temperature is evident in the ergotropy, which is consistently higher at zero temperature compared to nonzero temperatures, as shown in Fig. 3(a). As a result, at the end of charging, the ratio of effective $\eta = W_e/E_b = 0.917 \pm 0.017$ is higher at zero temperature compared to nonzero temperatures. Specifically, for the zero-temperature environment, the ergotropy is almost equal to the stored energy, while the ergotropy does not increase as the maximum stored energy for a nonzero temperature of environment. This is because the charging process of the battery at zero temperature is a unitary dynamics [67], so the energy stored in the battery can be completely extracted in the form of work [68].

It should be noted that the limitations on stored energy mentioned above arise from the disparity between the frequency of the charger-battery system and the frequencies of both the charger and battery, which is a result of the interaction between the battery and charger. To improve the stored energy, we adjust the frequency of the laser field to resonance with the global charger-battery system as $\omega_f = \omega - g_{cb}$. As shown in Fig. 3(b), both the stored energy and ergotropy of the battery have been significantly improved. It is to be noted that the ergotropy for the nonzero-temperature environment is lower than that for the zero-temperature environment, which is equal in principle. The difference here is due to the truncation of harmonic oscillator [68].

Although the stored energy can be increased by optimizing the laser frequency, it is required to probe the coupling constant between the charger and the battery. This requirement can be released by the catalyst-assisted charging process. As shown in Fig. 3(c), the performances of the catalyst-assisted charging protocol are similar to that of the direct charging with the optimized frequency of the external field. For example, both the stored energy and ergotropy for zero temperature are improved to 1.092 ± 0.011 and 0.872 ± 0.013, respectively. In addition, we test the performance of the catalyst by measuring the residual energy in the catalyst, which is the probability of occupying its excited state. At the end of the charging process with $t = 25$, the residual energy of the catalyst is 0.130 ± 0.003, which is quite small compared to both the stored energy and ergotropy.

Introducing an ancillary system will bring extra sources of noise, a typical example being the dissipation of catalyst.

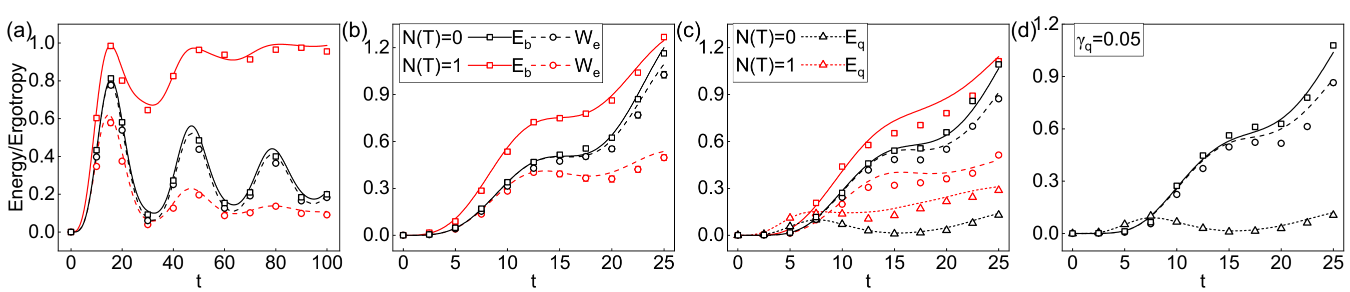

FIG. 3. Experimental results of energy and work for a QHOB performing two charging protocols at different temperatures. In the direct charging protocol, the stored energy E_b and ergotropy W_e of the QHOB for (a) $\omega_f = 1$ and (b) $\omega_f = 0.8$. In the catalyst-assisted charging protocol, the stored energy E_b and ergotropy W_e of the QHOB and the residual energy E_q of the catalyst for (c) $\gamma_q = 0$ and $\omega_f = 1$ and (d) $\gamma_q = 0.05$ and $\omega_f = 1$. Solid lines represent theoretical values and dots represent experimental values. The parameters for all panels are $\omega_c = \omega_b = 1$, $g_{cb} = g_{cq} = g_{bq} = 0.2$, $F = 0.1$, $\gamma_c = 0.05$. Error bars (smaller than the symbols) show statistical uncertainty from Monte Carlo simulations assuming Poissonian photon-counting statistics.

As shown in Fig. 3(d), when energy is dissipated from the catalyst to the environment with rate $\gamma_q = 0.05$, the maximum energy storage and ergotropy of the battery become 1.078 ± 0.009 and 0.865 ± 0.014, respectively. At the end of charging, the energy remaining in the catalyst is 0.105 ± 0.003. Since the energy of the catalyst is negligible, the dissipation of the catalyst does not have a significant effect on the performance of the battery [68].

Conclusion and discussion. In this Letter, we report experimental simulations of charging a QHOB in single-photon interferometric networks. Our experiment shows that when directly choosing the resonance frequency, there is an upper limit to the stored energy of the QHOB, which also results in an upper limit to the ergotropy. Furthermore, we demonstrate that these limitations can be broken by either optimizing the frequency of the laser field or introducing a catalyst system. Both methods significantly increase both stored energy and ergotropy of the QHOB without the requirement of choosing a specific charging time. In contrast, the catalyst-assisted charging protocol is more convenient since it does not require additional probing of the coupling constant between the charger and the battery. We have considered extending this method to the situation where multiple batteries are charged simultaneously, indicating that the advantages of catalysts are even more obvious [68]. Our experiment shows that there is no need to worry about the dissipation of the introduced catalysts, as it does not have a significant impact on the charging process.

Furthermore, from the viewpoint of experimental innovation, we design a general method for the realization of arbitrary nonunitary evolutions and the deterministic realizations of trace-preserving but not random unitary channels to characterize the evolution of the master equation. Our work is an experimental demonstration of the trace-preserving nonunitary quantum channel in a deterministic and general way, as well as an experimental demonstration of unlimited energy storage. The implementation method of the channel is universal and can be extended to arbitrary trace-preserving channels. Our experimental approach can be used to simulate a wider variety of quantum battery models.

Our results provide a convenient way to fully exploit the most significant advantage of the QHOB which is the ability to store unlimited energy. In contrast, for traditional batteries composed of two-level systems, it is needed to increase the number of two-level systems and exploit collective quantum resources [39]. In addition, the QHOB has another advantage in that the initial state of the whole system can be easily prepared in the ground state, thus eliminating the need for the initial quantum coherence of the charger [42]. Our work sheds light on the application of this advanced QB and paves different avenues for further research on QBs.

Acknowledgments. This work has been supported by the National Natural Science Foundation of China (Grants No. 92265209 and No. 12025401). H.Q.L. acknowledges support from NSFC (Grant No. 12088101). X.Z. acknowledges support from NSFC (Grant No. 12004184). D.K.Q. acknowledges support from NSFC (Grant No. 12305008) and the China Postdoctoral Science Foundation (Grant No. 2023M730198).

[1] J. D. Bekenstein, Phys. Rev. D **7**, 2333 (1973).
[2] J. M. Bardeen, B. Carter, and S. W. Hawking, Commun. Math. Phys. **31**, 161 (1973).
[3] J. Goold, M. Huber, A. Riera, L. del Rio, and P. Skrzypczyk, J. Phys. A: Math. Theor. **49**, 143001 (2016).
[4] S. Vinjanampathy and J. Anders, Contemp. Phys. **57**, 545 (2016).
[5] M. Horodecki and J. Oppenheim, Nat. Commun. **4**, 2059 (2013).
[6] F. G. S. L. Brandão, M. Horodecki, J. Oppenheim, J. M. Renes, and R. W. Spekkens, Phys. Rev. Lett. **111**, 250404 (2013).
[7] F. Brandão, M. Horodecki, N. Ng, J. Oppenheim, and S. Wehner, Proc. Natl. Acad. Sci. USA **112**, 3275 (2015).
[8] R. Alicki, M. Horodecki, P. Horodecki, and R. Horodecki, Open Syst. Inf. Dyn. **11**, 205 (2004).
[9] P. Skrzypczyk, A. J. Short, and S. Popescu, Nat. Commun. **5**, 4185 (2014).
[10] P. Ćwikliński, M. Studziński, M. Horodecki, and J. Oppenheim, Phys. Rev. Lett. **115**, 210403 (2015).
[11] M. Lostaglio, K. Korzekwa, D. Jennings, and T. Rudolph, Phys. Rev. X **5**, 021001 (2015).
[12] R. Alicki and M. Fannes, Phys. Rev. E **87**, 042123 (2013).
[13] F. C. Binder, S. Vinjanampathy, K. Modi, and J. Goold, New J. Phys. **17**, 075015 (2015).
[14] F. Campaioli, F. A. Pollock, and S. Vinjanampathy, in *Thermodynamics in the Quantum Regime: Fundamental Aspects and New Directions* (Springer, Cham, 2019), pp. 207–225.
[15] L. P. García-Pintos, A. Hamma, and A. del Campo, Phys. Rev. Lett. **125**, 040601 (2020).
[16] J.-Y. Gyhm, D. Šafránek, and D. Rosa, Phys. Rev. Lett. **128**, 140501 (2022).
[17] S. Seah, M. Perarnau-Llobet, G. Haack, N. Brunner, and S. Nimmrichter, Phys. Rev. Lett. **127**, 100601 (2021).
[18] M. Perarnau-Llobet, K. V. Hovhannisyan, M. Huber, P. Skrzypczyk, N. Brunner, and A. Acín, Phys. Rev. X **5**, 041011 (2015).
[19] J.-X. Liu, H.-L. Shi, Y.-H. Shi, X.-H. Wang, and W.-L. Yang, Phys. Rev. B **104**, 245418 (2021).
[20] H.-L. Shi, S. Ding, Q.-K. Wan, X.-H. Wang, and W.-L. Yang, Phys. Rev. Lett. **129**, 130602 (2022).
[21] M. Lostaglio, D. Jennings, and T. Rudolph, Nat. Commun. **6**, 6383 (2015).
[22] G. Francica, F. C. Binder, G. Guarnieri, M. T. Mitchison, J. Goold, and F. Plastina, Phys. Rev. Lett. **125**, 180603 (2020).
[23] R. Uzdin, A. Levy, and R. Kosloff, Phys. Rev. X **5**, 031044 (2015).
[24] J. Monsel, M. Fellous-Asiani, B. Huard, and A. Auffèves, Phys. Rev. Lett. **124**, 130601 (2020).
[25] F. Caravelli, B. Yan, L. P. García-Pintos, and A. Hamma, Quantum **5**, 505 (2021).
[26] G. Manzano, F. Plastina, and R. Zambrini, Phys. Rev. Lett. **121**, 120602 (2018).
[27] G. Francica, J. Goold, F. Plastina, and M. Paternostro, npj Quantum Inf. **3**, 12 (2017).

[28] G. Francica, Phys. Rev. E **105**, L052101 (2022).
[29] B. Çakmak, Phys. Rev. E **102**, 042111 (2020).
[30] S. Julià-Farré, T. Salamon, A. Riera, M. N. Bera, and M. Lewenstein, Phys. Rev. Res. **2**, 023113 (2020).
[31] T. P. Le, J. Levinsen, K. Modi, M. M. Parish, and F. A. Pollock, Phys. Rev. A **97**, 022106 (2018).
[32] D. Rossini, G. M. Andolina, D. Rosa, M. Carrega, and M. Polini, Phys. Rev. Lett. **125**, 236402 (2020).
[33] G. M. Andolina, M. Keck, A. Mari, V. Giovannetti, and M. Polini, Phys. Rev. B **99**, 205437 (2019).
[34] F. H. Kamin, F. T. Tabesh, S. Salimi, F. Kheirandish, and A. C. Santos, New J. Phys. **22**, 083007 (2020).
[35] F. Barra, Phys. Rev. Lett. **122**, 210601 (2019).
[36] D. Farina, G. M. Andolina, A. Mari, M. Polini, and V. Giovannetti, Phys. Rev. B **99**, 035421 (2019).
[37] S. Ghosh, T. Chanda, S. Mal, and A. Sen(De), Phys. Rev. A **104**, 032207 (2021).
[38] Y.-Y. Zhang, T.-R. Yang, L. Fu, and X. Wang, Phys. Rev. E **99**, 052106 (2019).
[39] D. Ferraro, M. Campisi, G. M. Andolina, V. Pellegrini, and M. Polini, Phys. Rev. Lett. **120**, 117702 (2018).
[40] F. H. Kamin, F. T. Tabesh, S. Salimi, and A. C. Santos, Phys. Rev. E **102**, 052109 (2020).
[41] F. Campaioli, F. A. Pollock, F. C. Binder, L. Céleri, J. Goold, S. Vinjanampathy, and K. Modi, Phys. Rev. Lett. **118**, 150601 (2017).
[42] G. M. Andolina, M. Keck, A. Mari, M. Campisi, V. Giovannetti, and M. Polini, Phys. Rev. Lett. **122**, 047702 (2019).
[43] A. Crescente, M. Carrega, M. Sassetti, and D. Ferraro, Phys. Rev. B **102**, 245407 (2020).
[44] G. M. Andolina, D. Farina, A. Mari, V. Pellegrini, V. Giovannetti, and M. Polini, Phys. Rev. B **98**, 205423 (2018).
[45] R. R. Rodríguez, B. Ahmadi, P. Mazurek, S. Barzanjeh, R. Alicki, and P. Horodecki, Phys. Rev. A **107**, 042419 (2023).
[46] N. Friis and M. Huber, Quantum **2**, 61 (2018).
[47] H.-P. Breuer and P. Francesco, *The Theory of Open Quantum Systems* (Oxford University Press, Oxford, UK, 2002).
[48] M. P. Müller, Phys. Rev. X **8**, 041051 (2018).
[49] N. H. Y. Ng, L. Mančinska, C. Cirstoiu, J. Eisert, and S. Wehner, New J. Phys. **17**, 085004 (2015).
[50] H. Wilming and R. Gallego, Phys. Rev. X **7**, 041033 (2017).
[51] N. Shiraishi and T. Sagawa, Phys. Rev. Lett. **126**, 150502 (2021).
[52] H. Wilming, Phys. Rev. Lett. **127**, 260402 (2021).
[53] K. Korzekwa and M. Lostaglio, Phys. Rev. Lett. **129**, 040602 (2022).
[54] J. Åberg, Phys. Rev. Lett. **113**, 150402 (2014).
[55] P. Lipka-Bartosik and P. Skrzypczyk, Phys. Rev. X **11**, 011061 (2021).
[56] P. Boes, J. Eisert, R. Gallego, M. P. Müller, and H. Wilming, Phys. Rev. Lett. **122**, 210402 (2019).
[57] M. Lostaglio and M. P. Müller, Phys. Rev. Lett. **123**, 020403 (2019).
[58] I. Henao and R. Uzdin, Quantum **5**, 547 (2021).
[59] A. E. Allahverdyan, R. Balian, and Th. M. Nieuwenhuizen, Europhys. Lett. **67**, 565 (2004).
[60] M. A. Nielsen and I. Chuang, *Quantum Computation and Quantum Information* (Cambridge University Press, Cambridge, UK, 2010).
[61] R. Penrose, *A Generalized Inverse for Matrices* (Cambridge University Press, Cambridge, UK, 1955).
[62] D. T. Pegg and S. M. Barnett, Phys. Rev. A **39**, 1665 (1989).
[63] S. A. Coon, M. I. Avetian, M. K. G. Kruse, U. van Kolck, P. Maris, and J. P. Vary, Phys. Rev. C **86**, 054002 (2012).
[64] M. Reck, A. Zeilinger, H. J. Bernstein, and P. Bertani, Phys. Rev. Lett. **73**, 58 (1994).
[65] W. R. Clements, P. C. Humphreys, B. J. Metcalf, W. S. Kolthammer, and I. A. Walmsley, Optica **3**, 1460 (2016).
[66] L. Xiao, K. Wang, X. Zhan, Z. Bian, K. Kawabata, M. Ueda, W. Yi, and P. Xue, Phys. Rev. Lett. **123**, 230401 (2019).
[67] A. Kossakowski, Rep. Math. Phys. **3**, 247 (1972).
[68] See Supplemental Material at http://link.aps.org/supplemental/10.1103/PhysRevB.108.L180301 for a detailed proposal of realization of arbitrary trace-preserving quantum channels and more numerical results of higher-dimensional QHOB.